Constraining the dextral component of slip on faults in the Tahoe basin using airborne and terrestrial LiDAR data

NEHRP grant G13AP00017 (IMW)

Graham Kent & Steven Wesnousky
Nevada Seismological Laboratory/0174
University of Nevada, Reno, Reno NV 89557

April 1, 2013 – June 30, 2014

Executive Summary: A reevaluation of active faulting across the Tahoe basin was conducted using a combination of airborne LiDAR (Light Detection and Ranging) imagery, high-resolution seismic CHIRP (acoustic variant, compressed high intensity radar pulse) profiles, and multibeam bathymetric mapping. In August 2010, the Tahoe Regional Planning Agency (TRPA) collected 941 square kilometers of airborne LiDAR data in the Tahoe basin. Our group was involved with data specification, contractor selection and data quality control. These data have a density of 11.82 points per square meter, with approximately 2 points per square meter striking the bare earth; the vertical accuracy of this dataset approaches 3.5 centimeters. The combined lateral and vertical resolution has refined the landward identification of fault scarps associated with the three major active fault zones in the Tahoe basin: the West Tahoe–Dollar Point fault, Stateline–North Tahoe fault, and Incline Village fault. By using the airborne LiDAR dataset, we were able to identify previously unmapped fault segments throughout the Tahoe basin, which heretofore were difficult to trace due to thick vegetation associated with rugged alpine terrain. Several lateral/medial moraines transected by faults were further investigated for potential piercing points to assess any lateral component of slip. Terrestrial LiDAR proved ineffective due to thick vegetation, including extensive manzanita bushes and conifer tress mantling the moraine crests (i.e., Cascade right-lateral). The airborne LiDAR imagery, however, confirms that potential fault-related lateral offsets across Tioga- and Tahoe-aged moraines do not appear to be progressive through time (i.e., accumulating slip), but instead highlights natural variability of geomorphic shape along morainal crests that can at times produce apparent lateral offset. Nonetheless, our new airborne LiDAR investigation highlights a much simpler mode of normal faulting in this western-most basin in the Walker Lane, in contrast to earlier investigations by Schweickert et al. (2004) and Howle et al. (2012) that have a much greater density of faults. Through integration of complementary geophysical datasets, we have developed a much-improved model of fault architecture and timing within the Tahoe basin. Our updated fault map provides a better understanding of the tectonics of the basin, and will help constrain future earthquake magnitudes and associated seismic hazards, such as ground ruptures and tsunamis.

Introduction and Rationale

Lake Tahoe occupies the westernmost basin within the trans-tensional Walker Lane deformation belt that abuts the eastern edge of the Sierra Nevada microplate (Unruh et al., 2003; Schweickert et al., 2004; Kent et al., 2005, Dingler et al., 2009, Brothers et al., 2009; Maloney et al., 2013; Busby, 2013). New geodetic surveys suggest that approximately 7 mm/yr, or about 15 percent of the total plate motion between the Pacific plate and the North American plate, is accommodated along this boundary near Lake Tahoe (Bormann, 2013); the majority of slip in this region of the northern Walker Lane is accommodated through dextral shear, although the exact distribution of this motion (e.g., strike-slip versus block rotation) remains unclear (Cashman and Fontaine, 2000; Wesnousky et al., 2012). Geodetic data suggest that the Tahoe basin accommodates equal amounts of extension and right-lateral shear (Hammond et al., 2011), but compelling evidence for the strike-slip component is sparse; the gradual opening-to-the-north geometry of the Tahoe basin, however, may suggest some form of left-lateral accommodation at the northern end of the basin.

Prior to acquisition of a basin-wide LiDAR dataset, mapping faults in the Tahoe basin was hampered not only by the presence of glacial deposits, but also by dense brush and forests, seasonal snow, and by the lake itself. Lindgren (1911) first recognized that the basin

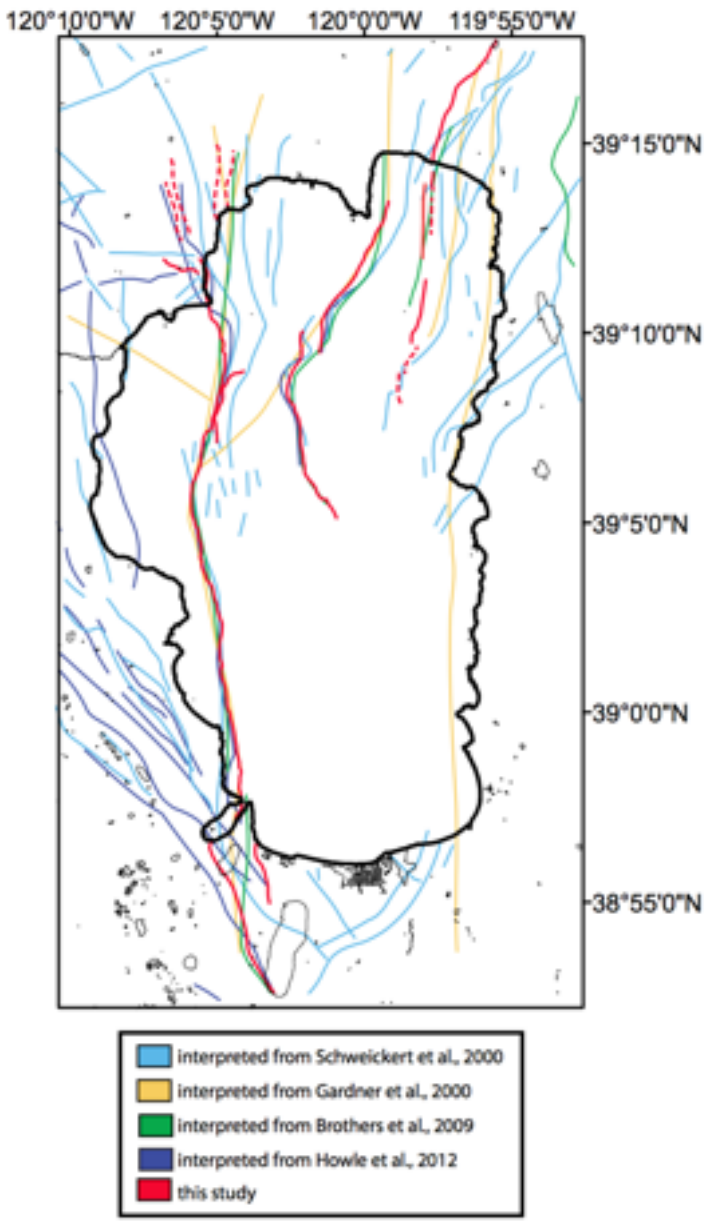

Figure 1 *A schematic diagram of fault density from various studies through time in the Lake Tahoe basin. The results from our study (red), highlight a simple right-stepping, en-echelon normal fault system that is in stark contrast to several previous fault studies (green, cyan), where fault densities are dramatically different. Also, previous faults such as the East Tahoe fault (gold, eastern shoreline) have been removed from our current map as no signature in either LiDAR or seismic profiling was found.*

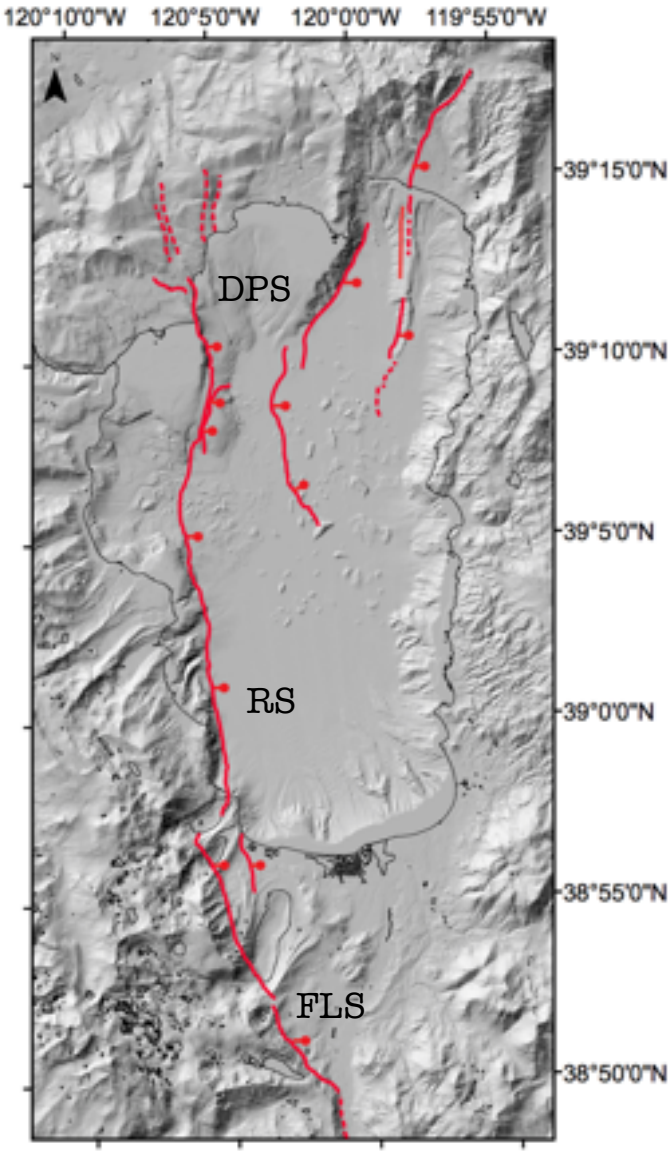

Figure 2 *Regional map of the Lake Tahoe basin that shows the LiDAR coverage of the entire basin as well as the locations of the observed faults (red). West Tahoe–Dollar Point fault (WTDPF), Stateline–North Tahoe fault (SLNTF), and Incline Village fault (IVF) are shown. Segmentation of the WTDPF is also highlighted. Debris from the McKinney Bay slide is evident as the blocky features located near the middle of the lake.*

bounding faults extend north into the Truckee basin. Additional work by Blackwelder (1933) and Birkeland (1963) continued to study the basin and its associated faults. Hyne et al. (1972) performed the earliest marine seismic studies in Lake Tahoe, providing the first views of fault architecture at the bottom of the lake. Gardner et al. (2000) provided further evidence of a right-stepping, en-echelon normal fault system through a comprehensive multibeam survey of Lake Tahoe. Schweickert et al. (2004) published the first comprehensive fault map of the entire basin showing numerous and complex faults. The many faults were particularly abundant near the mapped West Tahoe–Dollar Point fault (WTDPF) on the west side of the lake, as well as in the northern portion of the lake, coinciding with the Stateline–North Tahoe fault (SLNTF) and Incline Village fault (IVF). In contrast, faults mapped within lacustrine sediments using a sub-bottom CHIRP profiler in Lake Tahoe, Cascade Lake and Fallen Leaf Lake (Kent et al., 2005; Dingler et al, 2009; Brother et al., 2009; Maloney et al., 2013) presented a simpler view of faulting within the Tahoe basin. These lake-based maps, while clearly identifying the WTDPF, SLNTF and IVF, did not reveal the same complexity, or density of secondary faults (Fig. 1), as reported in the onshore fault maps published by Schweickert et al. (2004) and Howle et al. (2012). These

observations raised the following question: why is faulting observed on land so much more complex than that imaged in the lake? In principle, mapping faults and associated structures is rather straightforward in a lacustrine environment as observed in the Tahoe basin. Is there a geologic reason for this dichotomy? Perhaps mapping of faults on land provides a greater integration of time, thus being more sensitive to recording motion on faults with diminished slip-rates relative to the large basin bounding faults? Tahoe and Tioga glaciation may in fact work contrary to this notion, providing an excellent marker for late Pleistocene and Holocene fault movement, but in many cases may erase or inhibit mapping of older histories of rupture on land. Lastly, the mismatch between fault systems on land and in the lakes may simply be a misinterpretation in the geologic processes that shape the basin, resulting in incongruous maps. To this end, a comprehensive geophysical approach has been employed in both environments, outlined below, to attempt to resolve this issue and provide an updated fault map of late Pleistocene and Holocene rupture in the Tahoe basin, and test whether there is an obvious component of right-lateral slip on these faults, or newly discovered faults owing to the new capabilities of this LiDAR dataset.

Results:

In 2010, the Tahoe Regional Planning Agency (TRPA) commissioned Watershed Sciences to fly an airborne LiDAR survey of the Tahoe basin (Fig. 2). Our group was involved with data specification, contractor selection and data quality control. Though the TRPA commissioned the survey for land-use planning purposes, due to the high pulse density of the data active fault scarps across the basin could be easily identified. The flight paths and LiDAR instrumentation were designed to achieve a pulse density ≥ 8 pulses per square meter. Over 11 pulses per square meter were shot with approximately 2 strikes per square meter hitting the bare earth. Processing the resulting point cloud supported a 0.5-meter pixel resolution bare earth model of the Tahoe basin (Watershed Sciences, 2010), although data were resampled to 1 m grids. The raw LiDAR data were processed to remove the vegetation signal, resulting in a bare earth model suitable for geologic mapping purposes. After identifying faults scarps on the processed bare earth data, each trace was then verified through a field investigation. This process was further aided by fault exploration within the QPS *Fledermaus* 3-D interpretational environment that allows active slope shading of hill sides, and integration with other datasets, including multibeam bathymetric maps and seismic CHIRP profiles.

West Tahoe–Dollar Point fault

The West Tahoe-Dollar Point fault (WTDPF) bounds the western side of the Tahoe basin, starting in the south near Echo Summit, where it heads northwestward through Fallen Leaf Lake and

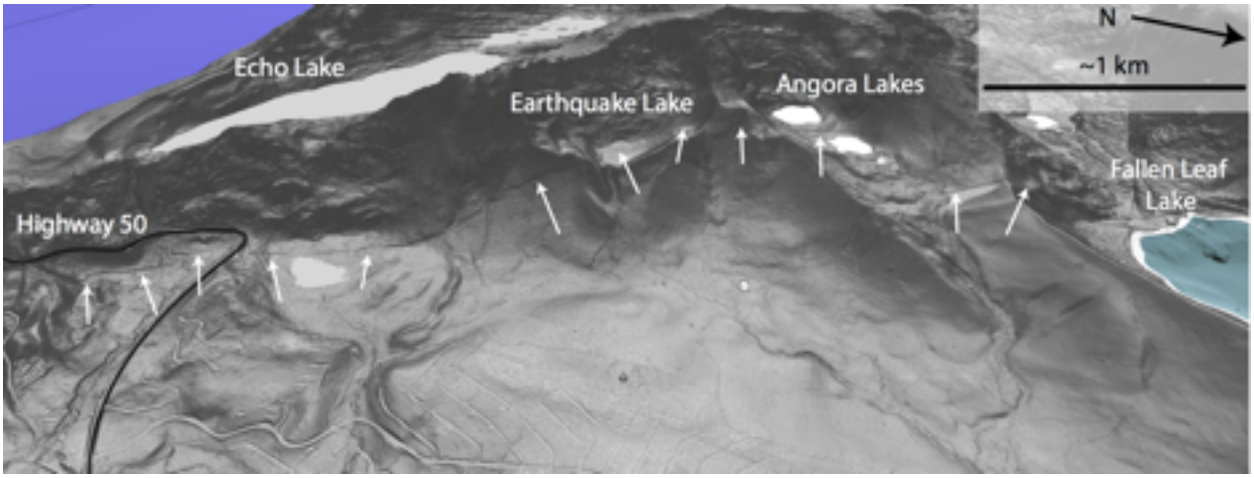

Figure 3 *A bare earth, slope-shade LiDAR image of the southern extent of the West Tahoe–Dollar Point fault from its southern terminus near Christmas Valley through to its descent into Fallen Leaf Lake. The scarp is clearly visible in the LiDAR imagery near Echo Summit where it then trends upward along the mountain front before cutting between the Upper and Lower Angora Lakes (see white arrows).*

Cascade Lake, then steps north into Lake Tahoe near Emerald Bay where it bounds the steep western escarpment offshore Rubicon. The WTDPF then traverses through McKinney Bay, reemerging onshore near Dollar Point. For clarity in discussing the WTDPF, it has been divided it into three segments. These are the Fallen Leaf Lake segment (FLS), the Rubicon segment (RS), and the Dollar Point segment (DPS). The locations of these segments are shown in Figure 2.

Fallen Leaf Segment

LiDAR imagery of the FLS of the WTDPF is shown in a 3-D perspective between Echo Summit and Fallen Leaf Lake (Fig. 3). As observed in Figure 3, the fault scarp is clearly visible south of Highway 50, where it dies out towards Christmas Valley. It continues northward, where it crosses Highway 50 and then skirts along the base of Flagpole Peak before climbing the side of Echo Peak. It then traverses across an ephemeral lake (also known as Earthquake Lake), and cuts between the Upper and Lower Angora Lakes before stepping into Fallen Leaf Lake. Previous work by Brothers et al. (2009) inferred that the FLS fault trace must be topographically lower (following a straight line) and lie in the valley at the base of Flagpole Peak as more obvious sections near Echo Summit and Angora Lakes were already identified in their study. Our analysis of the new LiDAR data indicates that portions of this fault are not confined to the base of the range front, but instead occasionally climb upslope. Though previous movement on the fault is undoubtedly responsible for Christmas Valley at the base of Flagpole Peak, the most recent movement appears to be encroaching westward, as is evidenced by fault scarps observed upslope. It should also be noted that there are several large stepovers along the fault, including a nearly one-half kilometer right step near Angora Lakes.

Figure 4 *Photograph showing the Fallen Leaf segment of the West Tahoe–Dollar Point fault scarp, where the fault cuts between the Upper and Lower Angora Lakes.*

A photo of the fault scarp as observed on the ground between the Upper and Lower Angora Lakes is shown in Figure 4. At this location, breaks in slope across the fault scarp may suggest multiple (potentially two or three) slip events with an offset of approximately two meters per event. Each potential event is characterized by a stair-stepping appearance. There is an obvious temporal component to weathering, as the top of the scarp has more weakly defined scarp faces, suggesting longer exposure to the elements. The top and bottom offset surfaces appear to be related to Tioga-aged glacial outwash, which resulted in a very flat surface that defines the total throw across the fault scarp with a maximum height of 6 meters.

North of Angora Lakes, the WTDPF scarp continues through the southern end of Fallen Leaf Lake, where it forms a large escarpment that is imaged in the multibeam sonar bathymetric dataset and vertical CHIRP cross-sections (Maloney et al., 2013; Brothers et al., 2009). Curiously, a second branch of the fault appears to form onshore just northwest of Fallen Leaf Lake and continue towards Baldwin Beach at Lake Tahoe (Figs. 2&5). It is difficult to determine how or if this branch continues south and connects up with the main strand of the fault. The main branch traverses near Mt. Tallac, where it crosses Cascade Lake (Fig. 5). The FLS is imaged as

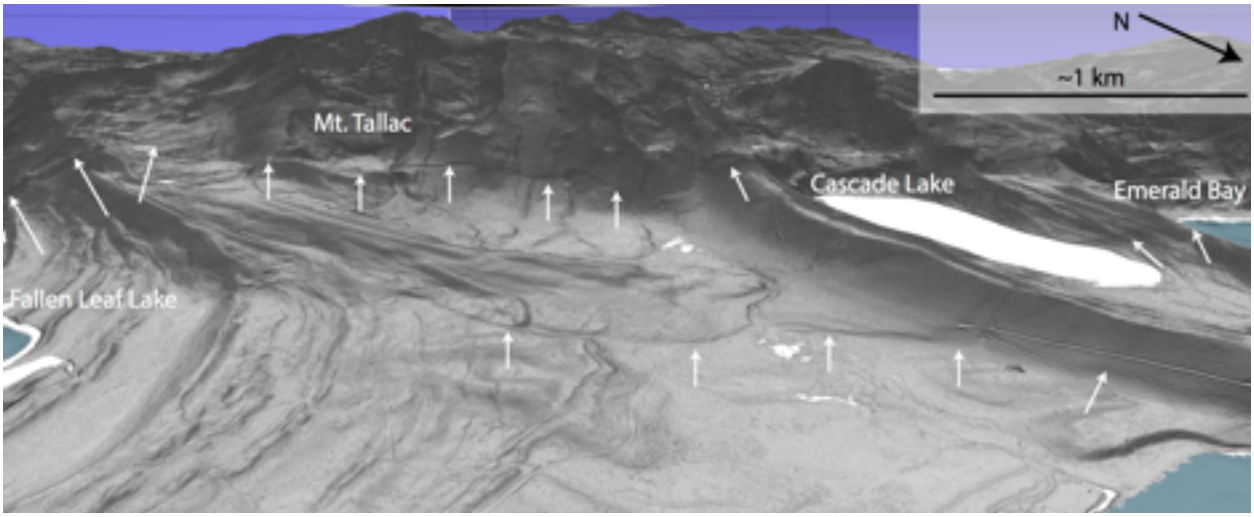

Figure 5 *A bare earth LiDAR image of the West Tahoe–Dollar Point fault near the vicinity of Mt. Tallac is shown. The fault scarp is clearly visible in the slope-shade LiDAR data, where it cuts along the face of Mt. Tallac and then crosses near the southwestern shore of Cascade Lake (white arrows). North of Fallen Leaf Lake, the fault also splays to the east and forms a second, fairly continuous trace toward Baldwin Beach in Lake Tahoe (lower set, white arrows).*

two distinct faults in Cascade Lake CHIRP data (Maloney et al., 2013). The main fault trace may continue a bit farther northwest, through a saddle in the moraine, and into Emerald Bay, where there is weak evidence from CHIRP profiling of stratal divergence towards the south (Maloney et al., 2013). However, clear evidence of a scarp in the LiDAR data is lacking between Cascade Lake and Emerald Bay. Maloney et al. (2013) suggests that the fault may continue on the east side of Fanette Island before stepping some 1.5 km towards the precipitous western edge of Lake Tahoe that defines the RS of the WTDPF. There is weak evidence for fault scarps continuing onshore to the northwest from southern Emerald Bay in the LiDAR data. Landslide scarps are observed approximately four kilometers north of Emerald Bay (Fig. 2). These features exhibit geomorphology typically associated with landslides such as arcuate head scarps, slump blocks and guide planes.

Rubicon Segment

The RS of the WTDPF is not observed on land, with the exception of a small slice of the fault and corresponding scarp observed on a flat bench near the northern entrance to Emerald Bay, which can be observed in the LiDAR dataset (Figs. 2&6). Continuing north, the fault trace plunges into the lake and follows the steep western wall of Lake Tahoe, which is observed in bathymetric and CHIRP data. This segment, extending from the mouth of Emerald Bay to the mid-section of McKinney Bay, is characterized by a steep, submerged escarpment, approximately 400 meters in height, and offsets a small fan delta at the base of the steep wall (Fig. 6). The fault scarp terminates abruptly at McKinney Bay, where the lakeshore shifts sharply to the west. This termination is a result of the McKinney Bay slide (Gardner et al.,

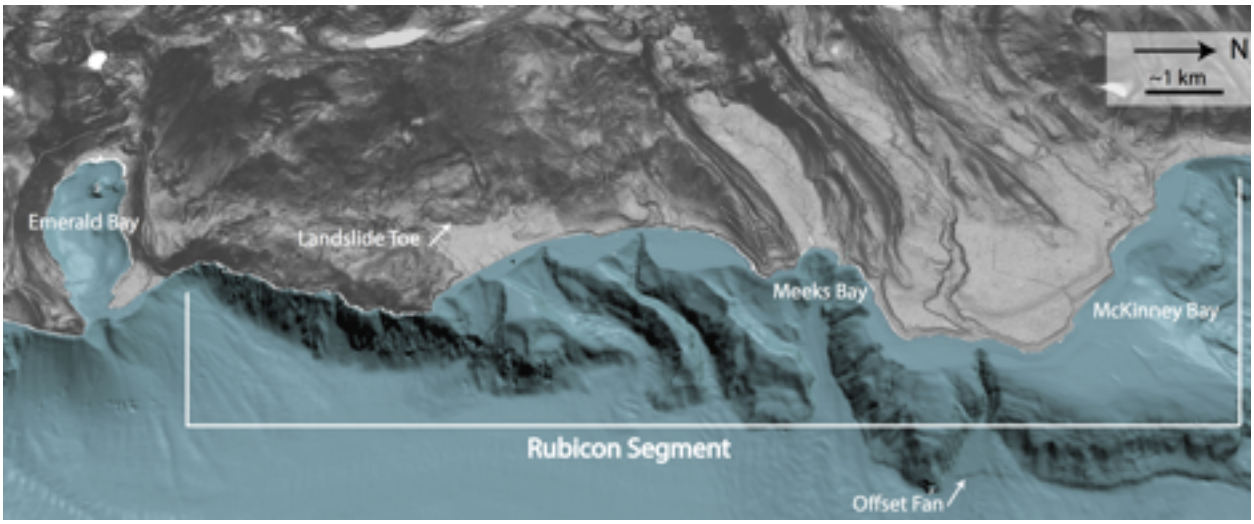

Figure 6 *Bare earth LiDAR model of the Tahoe- and Tioga-aged moraines south of McKinney Bay merged with swath bathymetry data from Lake Tahoe. Recent (latest Pleistocene or younger) faulting does not appear evident across these moraines. Older bedrock faulting may be present beneath these glacial deposits, though faulting of the character observed in this study along the southern portion of the West Tahoe–Dollar Point fault is not observed here. Note the offset of the fan-delta in the bathymetric dataset.*

2000), which has altered the shoreline and reduced the height of the fault-related escarpment. This megaslide (Fig. 2) is thought to be roughly 60 ka in age (Kent et al., 2005). Since this catastrophic event, smaller slides sourced to the west continue to mask the development of a continuous fault scarp (Smith et al., 2013). In the LiDAR data, recent (Holocene or younger) faulting does not appear to offset the onshore moraines between Emerald Bay and McKinney Bay (Fig. 6). The north-facing slopes on General–Meeks and McKinney–General moraines have well developed recessional moraines that are preserved on the steep, north-facing slopes and are linear in form. Older bedrock faulting may be present beneath the moraines, but faulting of the character observed from the southern portion of the basin, and in other sedimentary areas is not observed here. It should be noted that the apparent northern segment boundary of the RS or change in relief across the scarp is a consequence of the McKinney Bay slide (Fig. 2), in contrast to the nearly 1.5 km stepover between the FLS and RS of the WTDPF.

Dollar Point Segment

Beyond McKinney Bay, the WTDPF again follows submerged topography, this time through a shallow, offshore shoal (Fig. 1). In this location, the topography has both a more gentle and blunt slope. The scarp, instead of forming a steep wall as it does to the south, is less strongly developed to the north. A secondary splay just to the east near this bench may help distribute some of the tectonic strain, although due to the short length of this structure, it is likely minor in comparison to the transfer of slip to the other northeasterly faults, including the Stateline–North Tahoe fault and Incline Village fault.

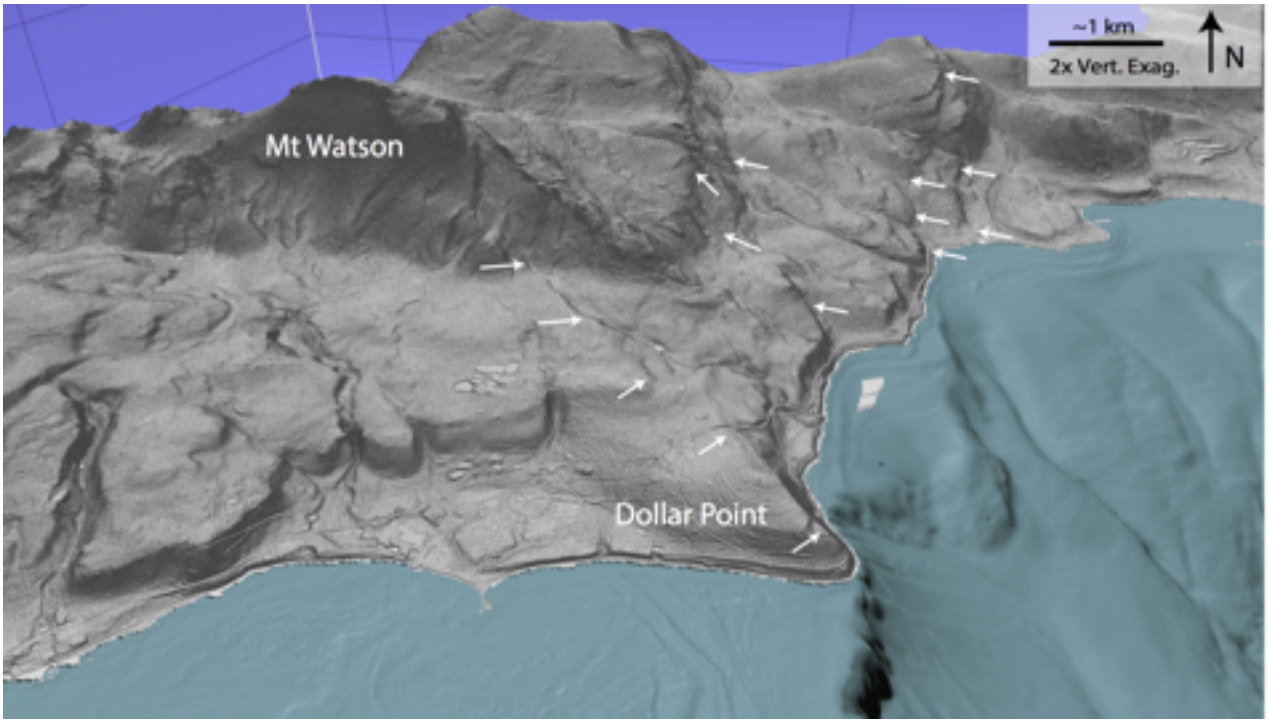

Figure 7 *Bare earth LiDAR model of the Tahoe basin near Dollar Point is shown. At this location, the orientation of the West Tahoe–Dollar Point fault changes from a north-northwest trend to a predominantly west-northwest trend. The fault appears to be dying out northwest of Dollar Point (white arrows), although it may be influenced by the Polaris fault zone further to the northwest.*

The DPS scarp is also observed onshore in the LiDAR data. At Dollar Point, the DPS splays into at least three, poorly defined, west-northwest and north–northwest trending fault traces (Fig. 2). The fault scarps, measured both from the LiDAR as well as from field investigation, are approximately 15 to 20 m high for the west-northwest trending structure and significantly higher (~30 m or more) for the more northerly oriented fault scarps. The high offset for both scarps suggests that they record multitude of rupture events (Fig. 7). The more northerly oriented features are formed in more competent rock and may integrate a much longer span of time in relation to many other scarps observed within the basin that are likely reset by either Tahoe- or Tioga-aged glaciation.

Scarp heights along the west-northwest trending structure decrease to the northwest and we do not observe a strongly developed main fault trace in LiDAR data. This type of geometry is characteristic of what occurs near the ends of a fault as strike orientation can change dramatically. However, the orientation of the north-northwestward trending DPS scarps is spatially correlative to the newly identified Polaris Fault zone (Hunter et al., 2011). Therefore, the possibility exists that the DPS of the WTDPF is bleeding into the Polaris fault zone,

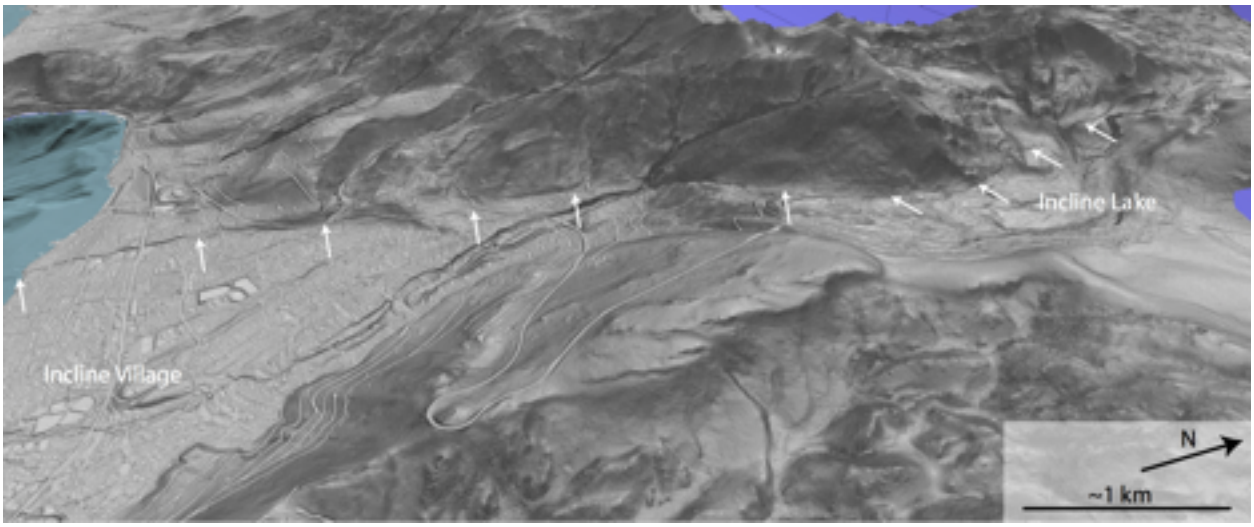

Figure 8 *Bare earth LiDAR model highlighting the Incline Village fault is shown. The southern terminus of this fault extends some 10 kilometers into the lake. Onshore, the Incline Village fault traverses through neighborhoods before trending north-northeastward up the Mt. Rose Highway corridor, where it dies out to the west of the former Incline Lake dam abutment (white arrows).*

highlighting a transition from a mostly normal fault system, into one that is more characterized by right-lateral strike slip faulting.

Incline Village Fault

The Incline Village fault (IVF) is traced in Lake Tahoe along a prominent spine from the shoreline to full water depth, and is roughly parallel to the Stateline–North Tahoe fault (SLNTF, Fig. 2). The fault extends north of the lakeshore, parallel to the Mt. Rose highway corridor, to slightly north of the manmade Incline Lake. In Lake Tahoe, CHIRP profiles indicate the main fault trace is normal, down-to-the-east; some synthetic east dipping faults are observed in the vicinity of a small stepover in fault structure near the shoreline. Dingler et al. (2009) observed an offset boulder layer that provides evidence for ~14 meters of vertical deformation across the fault since the Tahoe glaciation. Paleoseismic trenching onshore indicates the most recent rupture of this fault occurred ~500 years B.P. (Seitz et al., 2005).

The nearshore and onshore component of the IVF, is a north-south striking normal fault that continues northward through the community of Incline Village before terminating near the base of Relay Peak, just to the northwest of Incline Lake (Fig. 8). The fault scarp is clearly visible throughout the community where the fault emerges near the lake, crosses Lakeshore Blvd, and continues parallel to South/North Blvd, where it is clearly visible behind the former Incline Village Elementary School. At this point, the fault scarp is approximately 8 meters in height.

North of Incline Village, the fault continues along the south side of a subsidiary flank of Relay Peak. The fault scarp is clearly evident on the ground in this location. Near the vicinity of Incline Lake (Fig. 8), the fault jogs west and climbs Relay Peak, away from Incline Lake. Near this location, the scarp is approximately 2-4 meters high. Again, the fault can be traced on the ground in this location. Near Incline Lake, there is significant historical anthropological disruption of the ground surface. This disruption includes ground terraces and cuts, which are evidence of road building and dam development. This disruption makes tracing the fault more difficult on the ground, nevertheless, the fault is clearly evident in the LiDAR data.

Discussion:

Fault Density and Architecture

The primary purpose of our study was two-fold: (1) to identify the location of active faults in the Tahoe basin, recorded within late Pleistocene– and Holocene–aged deposits, using the latest arsenal of sophisticated mapping tools (i.e., LiDAR, seismic CHIRP profiling and multibeam sonar); (2) to find potential piercing points that may give constraints on any right-lateral (or left-lateral) motion on the major normal faults within the basin, and/or newly discovered faults. The application of airborne LiDAR to the Tahoe basin was a critical step in helping to resolve the disparity in fault architecture as reported from terrestrial mapping (Schweickert et al., 2004) and within lakes using sub-bottom sonar mapping techniques (e.g., Dingler et al., 2009, Brothers et al., 2009). At first glance, the lake studies provide what appears to be a relatively simple architecture, with a system of three en-echelon, right-stepping, down-to-the-east normal faults, and little evidence for a multitude of associated fault structures. This appears to be in conflict with the Schweickert et al. (2000; 2004) fault map, and further refinement by Howle et al. (2012), which used an earlier Army Corps of Engineers LiDAR survey that show a plethora of fault structures on land (Fig. 1). These terrestrial fault maps are incongruent (in terms of density) with the fault maps derived from offshore multibeam bathymetry and seismic CHIRP data. The most notable difference is along the west shore of Lake Tahoe, where the Tahoe-Sierra frontal fault zone has been mapped as a series of four closely spaced faults with a NW-SE orientation near Meeks Bay (e.g., Howle et al., 2012). Integrated extension across this zone is reported to be nearly 1.5 mm/yr of down-to-the east normal motion, which is more than twice the observed WTDPF rate, which is largely responsible for the deep basin that forms Lake Tahoe (Dingler et al., 2009). This region of the basin is characterized by three to four prominent lateral moraines from glaciers sourced in the Desolation Wilderness, and are composed of pre Tahoe-, Tahoe– and Tioga–aged material (Howle et al., 2012).

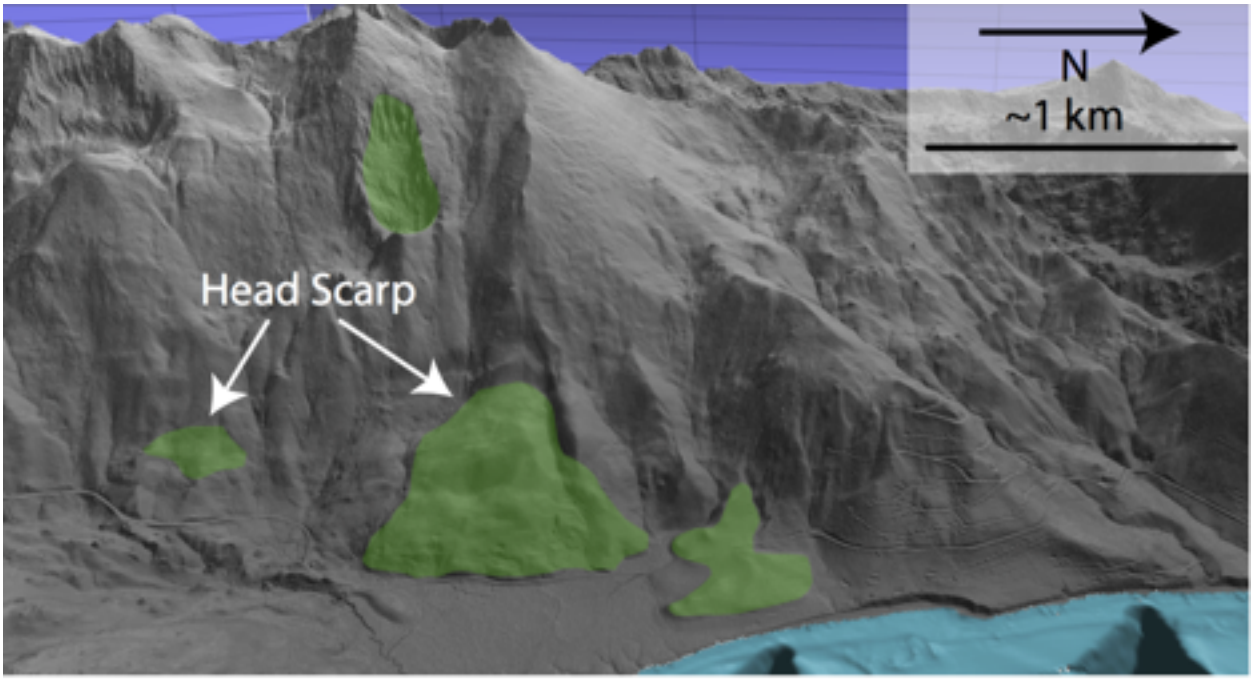

Figure 9 *Bare earth LiDAR imagery shows features interpreted to be landslides (shown in green) and their associated head scarps just north of Emerald Bay. The terrain in this area is highly susceptible to landslides.*

The most striking observation from the 2010 Watershed Sciences bare-earth LiDAR data is the high-resolution imaging of the terrestrial portions of the WTDPF and IVF active fault scarps. Slope shaded digital elevation maps (DEM) clearly highlight fault scarps in a variety of terrains that include flat lying regions, steep hillsides, and across lateral moraines. The FLS of the WTDPF provides a template for fault identification in other regions of the basin given the multitude of landforms that are offset by this segment. Although the WTDPF fault trace south of Fallen Leaf Lake appears rather straightforward in terms of structural complexity, aside from a nearly one-half kilometer stepover near Angora Lakes, it also has a curious behavior of climbing up the steep hillside near Earthquake Lake. This observation implies some level of reorganization of slip as the fault has abandoned its position at the base of the range front. In contrast, north of Fallen Leaf Lake, the FLS of the WTDPF appears to break into two separate strands, one maintaining its position near the edge of the range front, the other outboard toward Lake Tahoe, where the LiDAR data suggests that it enters the lake west of Baldwin Beach. This level of fault complexity may play an important role in the transfer of strain across the relatively large 1.5 km right-stepover between the FLS and RS of the WTDPF.

Onshore north of Emerald Bay, in the region of Rubicon and Meeks Bay, through-going structures, similar to those found along the FLS of the WTDPF are lacking. There is some hint of what appears to be a fault-like structure emerging from the central portion Emerald Bay

heading to the north, but careful analysis suggests it may owe its existence to mass-wasting of material downslope (Fig. 9). North of these landslide features, the moraines near Meeks Bay appear to be devoid of any clear offset features that show linearity and/or continuity from moraine crest to moraine crest. Unlike faulted moraines along the FLS of the WTDPF, the slopes of the moraines in this area appear devoid of any obvious fault scarps. If through-going structures along the Tahoe-Sierra frontal fault system exist as purported by Howle et al. (2012), then it is difficult to explain why they were not easily imaged in the LiDAR data, given the clear imaging of ruptures along the FLS of the WTDPF. Both PIs (Kent and Wesnousky) have walked the moraine crests both north and south of Emerald Bay to understand the features mapped by both Schweichert et al. (2004) and Howle et al. (2012).

The most complicating factor along the northern stretch (Dollar Point segment) of the WTDPF is that several splays integrate across more competent material, and thus, may record a longer period of slip that those regions that have been "reset" by Tahoe and Tioga glaciation. The observed horsetailing of fault structure, including dramatic changes in azimuth, are consistent with terminations of normal faults systems (Faulds et al., 2011).

Kinematically, changes in fault location as well as the continual opening of the basin may be related to a slight counter-clockwise (CCW) rotation or pivot along the eastern edge of the Sierra Nevada microplate. This rotation would drive the basins to open northward through time as observed in the overall morphology of the Tahoe basin. This change in microplate dynamics may be relatively recent based on evidence from the geomorphology of the SLNTF. The scarp height diminishes almost instantaneously where it steps onshore at Crystal Bay. South of the 400 m scarp, on the floor in Lake Tahoe, scarp height varies from on-order 10 m in height to barely visible due to either diminished slip and/or sedimentation rate outpacing accommodation. One can invoke a long-term history of diminished slip along the southern extent of the SLNTF that has greatly muted the fault scarp height, or perhaps a model where recent propagation of the SLNTF toward the south where it dies mid-lake, helps to "open" the basin northward. In this model, the DPS of the WTDPF has diminishing slip over this time period, as more and more slip has been transferred over to the southward propagating SLNTF.

Tahoe–Sierra Frontal Fault Zone

Research published in the early 2000's by Howle (2000) and Schweickert et al. (2004) commented that the NW-SE-oriented Tahoe-Sierra frontal fault system is a "complex zone which includes numerous subparallel, steeply east-dipping faults with apparent east-side-down normal displacement" and "carefully documented sinistral oblique displacements along several faults

cutting glacial moraines along Meeks Creek southwest of Meeks Bay." Recently, a subset of authors published an update to their previous work (Howle et al., 2012) that provides more detailed evidence (through the use of 2008 Army Corps airborne LiDAR) of normal motion (1.5 ± 0.4 mm/yr) along the frontal fault system, but there wasn't any further discussion of sinistral (or dextral) motion along this fault zone. Instead, Howle et al. (2012) highlighted the tectonic geomorphology of faulted lateral/medial moraines to include side-slope troughs, back-titled moraine crests, triangular-faceted moraine scarps, and extensional fault-propagation folds in lateral/medial moraines (or "blind normal faults"). Their approach was to use indirect indicators of fault motion (e.g., back tilting of moraine crests) if obvious geomorphic features such as scarps were lacking. South of Emerald Bay, faults mapped by Howle et al. (2012) are in general agreement with this study regarding location, as scarps are prominent, continuous features, cross lateral/medial moraines, and are imaged either atop the crest and/or on the sides of the steepened moraines.

North of Emerald Bay, there remains a strong disagreement on the existence of the Tahoe–Sierra frontal fault system, which provides two dramatically different views on the fault architecture of the Tahoe basin: Howle et al. (2012) argue that the Tahoe–Sierra frontal fault system connects with our FLS segment of the WTDPF to provide a longer frontal fault system at the expense of a shortened WTDPF. This disagreement has profound implications on fault length, maximum earthquake magnitude, and time evolution of basin formation. Our research suggests the FLS of the WTDPF steps into the lake some 1.5 km northeast, linking up with the RS of the WTPDF; this stepover zone is made somewhat more complex by the identification of a second active strand just north of Fallen Leaf Lake that trends roughly northwest to north, moving offshore just west of Baldwin Beach. Our preferred model keeps slip-rates somewhat in check along the entire 55-km-long WTDPF, from the FLS to the DPS, with vertical rates ranging somewhere near 0.4-0.8 mm/yr (Dingler et al., 2009; Brothers et al., 2009). The Howle et al. (2012) model has 2 times greater vertical slip across the frontal fault system than observed on the WTDPF; this observation is at odds with basin morphology in that the WTDPF is the basin-bounding fault system responsible for much of the accommodation that formed the lake. Thus, for the Howle et al. (2012) model to be valid, it would require the frontal fault system to be a nascent one, otherwise the shoreline of yet a deeper lake would be shifted to the west coincident with a long term normal faulting history along the Tahoe–Sierra frontal fault system. Also, within a larger Tahoe–Sierra frontal fault system, slip-rates would nearly triple north of Emerald Bay, and yet fault signatures across the glacial moraines, as manifested by scarps, are much more subdued.

The use of indirect evidence for mapping faults across moraines is not without merit. For example, a well-exposed fault scarp near the Angora Lakes parking lot is located within a 35-m-deep saddle, or depression, that cuts through the lateral moraine that bounds Fallen Leaf Lake to the west . Assuming a Younger Tahoe age of approximately 70 ka (Howle et al., 2012) and a slip-rate of 0.5 mm/year (within the range reported by Brothers et al., 2009 at Fallen Leaf Lake), then one can roughly calculate some level of parity between these observations. Maloney et al. (2013) mapped the FLS of the WTDPF transitioning through the southern third of Cascade Lake, where it begins to horsetail into a handful of splays upon exiting the western shoreline. Thereafter, the fault moves westward towards Emerald Bay, possibly dying out, but not before contributing to a complex 25-m notch in the medial moraine (likely modified through erosion). Although the fault scarp here is not a clean as seen near Angora Lakes, the dramatic expression of the scarp plunging into Cascade Lake from the east, combined with CHIRP imagery within Cascade Lake, provides some level of confidence that the fault has interacted with the medial moraine that separates Cascade Lake and Emerald Bay to the west.

It is clear that not all notches, changes in slope, and other indirect structures observed within moraines require faulting to produce the range of geomorphologic expressions observed in glacial terrains world-wide. If more direct indicators for fault movement are missing, or are at least ambiguous, how does one determine whether the feature in question is due to faulting, or just the imperfect construction of a moraine, further modified through time by erosion and /or slumping? If these features are due to coherent faulting, one would expect that these features might be continuous from ridge crest to ridge crest with some level of linearity. Along this trend, a subsection of the fault might have a well-formed scarp that would aid in its identification. Absent linearity and any noticeable subsections containing an unambiguous scarp, interpretation becomes much more difficult. This can be made even more difficult by the presence of landslides that may produce scarps sourced through the process of mass wasting.

As previously mentioned, interpretations diverge north of Emerald Bay as one approaches the moraines that are found near Meeks Bay. Howle et al. (2012) identify a fault scarp emerging near the center of Emerald Bay, then wrapping around the range front and identified as the Rubicon Peak fault zone. We also observe a system of scarps that extends some 4 km north of Emerald Bay, but a 1.5-kilometer-wide section may provide clues to their origin. The central piece is arcuate in shape and has many of the characteristics of slope failure, such as a noticeable head scarp, U-shaped scars, and slumps. Other examples of slides are observed both above this feature, and actually within the slide itself. There are also countless examples of slope failure observed in the LiDAR data between Emerald Bay and McKinney Bay, including a handful of

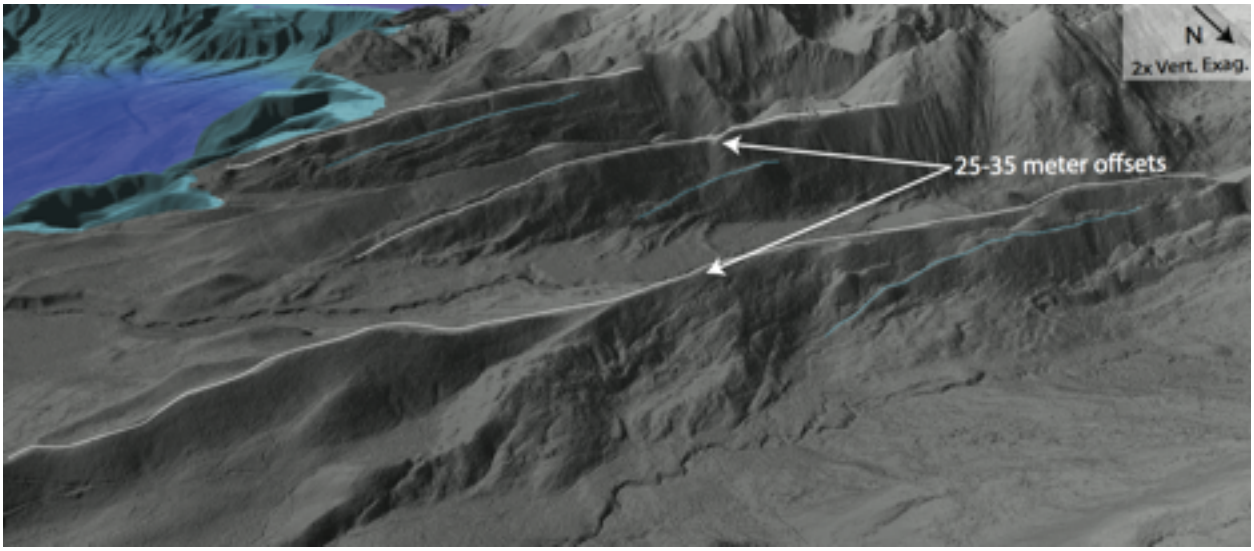

Figure 10 *Bare earth LiDAR imagery shows the Meeks Creek moraine complex. White lines represent the moraine crests and blue represents other linear features (recessionals) on the north faces of the moraines. Notches observed in the moraine crests are measured, though similar or scaled offsets are not observed within other linear features on the side of the moraines. Linear continuity between the notches or across all moraines is not readily observed, nor is there evidence for faulting on the slopes or the valleys between the moraines.*

large slides near Ellis Peak. Our interpretation is that the Rubicon Peak fault zone is more likely associated with mass wasting, not movement on a fault Moving north, there are several prominent lateral and medial moraines near Meeks Bay, including Meeks Creek, General–Meeks, McKinney–General and McKinney moraines (after Howle et al., 2012). Slopes of this moraine complex do not perfectly grade toward the lake, and notches and "back-tilting" of the moraine crest, in several places are highlighted by Howle et al. (2012). The largest of the recognized facets is on-order 25 m in height (Fg. 10). There is also some evidence for dextral offset (or apparent offset) of a likely Tioga-aged ridge crest along the General–Meeks moraine at the location of one of the largest facets, but it is difficult to extrapolate this feature, at least in a right-lateral sense, to either Meeks Creek or McKinney–General moraines. This lack of continuity gives pause with regards to any sustained fault trend; in the Howle et al. (2012) model, the largest facets do not connect from moraine to moraine causing significant swings in slip-rates over distances less than 2 km. Instead, some form of linearity is maintained at the expenses of consistency of slip-rate over short distances. Thus, the only other potential forms of continuity would be the facets and breaks in slopes that might reveal a more continuous system below. Again, several facets are 10s of meters in height that would require (locally) an approximate 0.35 mm/yr vertical slip-rate if offsetting Younger Tahoe moraines as postulated by Howle et al. (2012). Summed across several notches down the ridge crest, provides an integrated vertical slip-rate that is about 1.5 mm/yr. If the older moraines have been misidentified and are of Older Tahoe age, then slip-rates would be nearly halved. If the offset facets are indeed Younger

Tahoe-aged, and the recessional moraines are Tioga-aged, then the side-wall linear ridges of the recessional moraines should have about one-fifth the accrued displacement relative to the Tahoe-aged features—or about 5 meters (Fig. 10). And yet, these linear features do not appear to show that degree of deformation within the LiDAR dataset; at best there's a few meters of chatter along these linear features. This observation decreases confidence that these indirect indicators of slip are a useful proxy for fault slip in this particular area.

The moraines of Meeks Bay, however, do exhibit some curious behavior. While slip-rate estimates do not seem consistent when comparing Tahoe- and Tioga-related features, nonetheless there are several identifiable scarps across this complex. Mass wasting is common to the Tahoe basin as evidenced by submarine slide deposits (Smith et al., 2013; Maloney et al., 2013), and the McKinney Bay landslide (Gardner et al., 2000), which exemplifies an extreme geologic event. The quadrant extending from Emerald Bay to McKinney Bay appears very prone to landslides, and one can obviously extend this northward where remnants of the McKinney Bay slide are sitting at the bottom of the lake. One possibility that would allow Tahoe-aged features to be offset, while Tioga-aged features remain intact, would be a large landslide, potentially associated with the McKinney Bay failure, where a southern sliver of the failure lurched forward, but only partially failed. Although highly speculative, the 2010 LiDAR dataset may have provided clues to the location of a potential megaslide, if and when, a second event similar to the McKinney Bay slide takes place. That said, there appears to be a chaotic mixture of offsets on inferred Tahoe- and Tioga-aged moraines making it difficult to piece together a coherent history of either slip or sliding.

Dextral slip?

The number of obvious locations to test for a strike-slip component to any of the large normal faults in the Tahoe basin was minimal: the two best candidates where near Angora and Cascade Lakes. Unfortunately, both locations were choked with manzanita brush and/or pine trees that made terrestrial LiDAR scanning with our I-site 8800 unit impractical (although we tried). The best geometry as seen from airborne LiDAR was seen on the ridge southeast of Cascade Lake (Fig. 11). The likely Tahoe- and Tioga-aged aged features show progressive vertical offset through time, which is encouraging with respect to obtaining vertical slip-rates (Fig. 12). Lateral offsets where not apparent, and "creative" interpretations of the sinuous behavior only resulted in slip-rates that reversed (i.e., left-lateral) back tthrough Tahoe time. Thus, it is more likely that the amount of strike-slip motion is negligible through time, and the West Tahoe–Dollar Point fault is simply a normal fault.

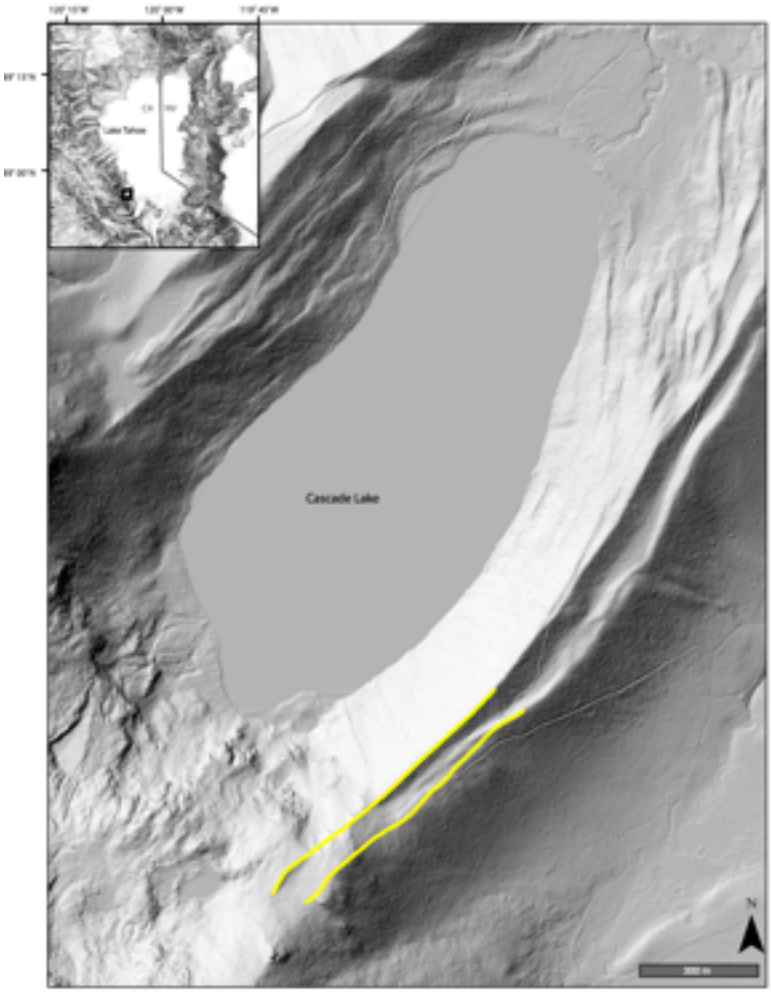

Figure 11 *Bare earth LiDAR imagery of the right-lateral moraine at Cascade Lake, with the Tahoe– (right-yellow) and Tioga–aged (left-yellow) moraine crests noted.*

Conclusions

Prior to the 2010 LiDAR survey, the fault complexity on land appeared higher than that observed in Lake Tahoe. Previous work in Lake Tahoe (Brothers et al., 2009; Dingler et al., 2009) clearly showed evidence for relatively simple fault geometries within the deepest part of the basin. These results were inconsistent with work published by Schweickert et al. (2004) and Howle et al. (2012), who documented very complex fault geometries on land. We argue that the fault geometry on land is less complicated than previously thought and that it more consistent with the fault geometry imaged within Lake Tahoe. The combined approach of this study clearly shows the locations of the major active faults in the Tahoe basin. Between the newly acquired LiDAR data and the addition of the new CHIRP and multibeam data, the normal faults have been mapped both onshore and within lakes.

Analysis of LiDAR data between Emerald Bay and Meeks Bay highlights the complexity of this quadrant of the lakeshore, with significant evidence for mass wasting. Although the moraine crests of Meeks Bay show a degree of complexity, through-going structures are difficult to identify; correlation of potential Tahoe-age triangular facets and back-tilted slopes from moraine crest to moraine crest is somewhat possible, Tioga-age recessional moraines preserved on the north slopes of these moraines do not show corresponding offsets (about 1/5th displacement), which is inconsistent with a fault-based origin. Instead, we speculate that some of these features may be related to mass movement associated with the McKinney Bay slide or other mass wasting events. The few candidate piercing points in the basin along faulted lateral moraines near Angora and Cascade lakes do not show progressive offset between Tioga- and Tahoe-aged

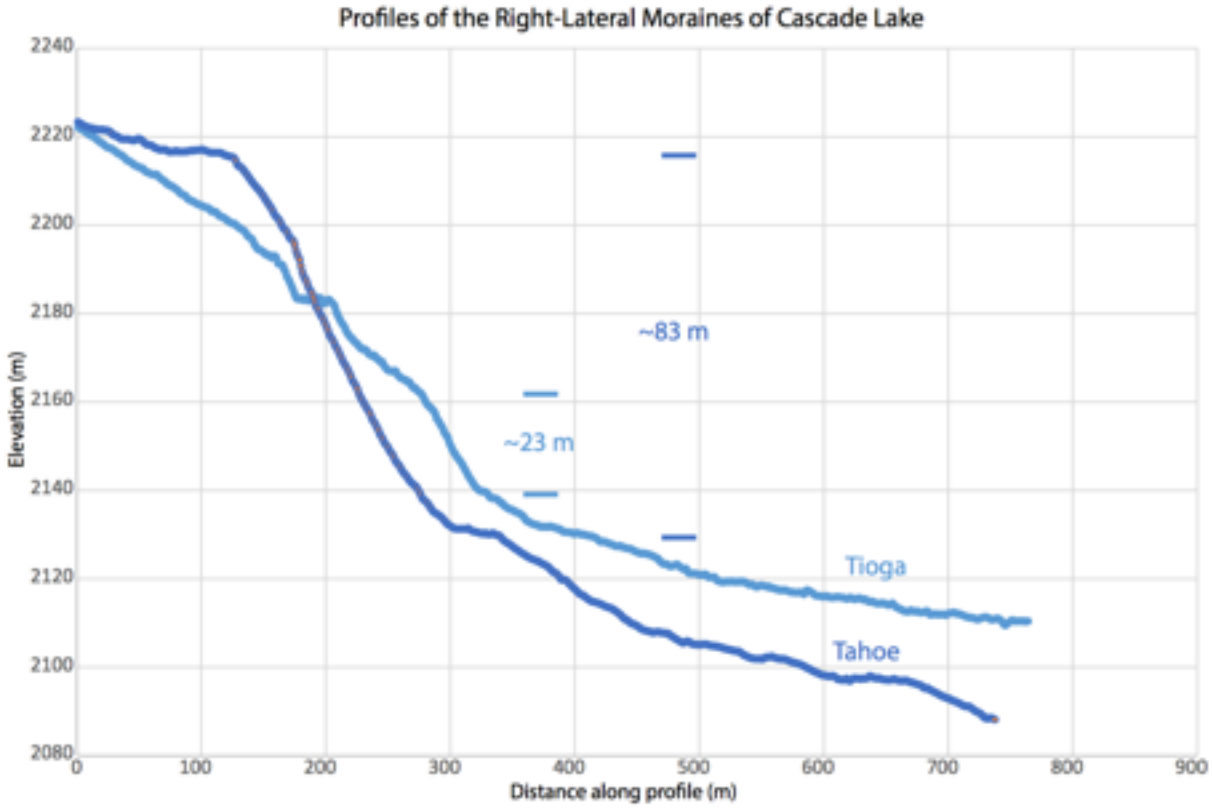

Figure 12 *Profiles along crest of Tahoe-(blue) and Tioga-aged (cyan) moraines (Fig. 11), highlighting progressive vertical offset (~ 1 mm/yr) through time, assuming a Younger Tahoe date for this feature.*

features; instead, likely natural variability of geomorphic shape provide inconsistent offsets that are not consistent with any right lateral motion.

References

Birkeland, P.W., 1963, Pleistocene volcanics and deformation of the Truckee area, north of Lake Tahoe, California, *Geol. Soc. America Bull., v. 74*, p. 1453-1464.

Blackwelder, E., 1933, Eastern slope of the Sierra Nevada, *16th Internat. Geological Cong., Guidebook 16*, p. 81-95.

Bormann, J. M., 2013, New Insights into Strain Accumulation and Release in the Central and Northern Walker Lane, Pacific-North American Plate Boundary, California and Nevada, USA [Doctorate Dissertaion]: Univerist of Nevada, Reno, 150 p.

Brothers, D. S., Kent, G. M., Driscoll, N. W., Smith, S. B., Karlin, R., Dingler, J. A., Harding, A. J., Seitz, G. G., and Babcock, J. M., 2009, New constraints on deformation, slip rate, and timing of the most recent earthquake on the West Tahoe-Dollar Point Fault, Lake Tahoe Basin, California: Bulletin of the Seismological Society of America, v. 99, no. 2A, p. 499-519.

Busby, C. J., 2013, Birth of a Plate Boundary at ~12 Ma in the Ancestral Cascades Arc, and implications for transtensional rift development, Walker Lane belt, Geol. Soc. Am. Bull., 9,(5) 14pp., doi:10.1130/GES00928.

Cashman, P. H., and S. A. Fontaine, Strain partitioning in the northern Walker Lane, western Nevada and northeastern California, *Tectonophysics*, **326**, 111–130, 2000.

Dingler, J., Kent, G., Driscoll, N., Babcock, J., Harding, A., Seitz, G., Karlin, B., and Goldman, C., 2009, A high-resolution seismic CHIRP investigation of active normal faulting across Lake Tahoe basin, California-Nevada: Geological Society of America Bulletin, v. 121, no. 7-8, p. 1089-1107.

Faulds, J. E., Hinz, J.H., Coolbaugh, M.F., Cashman, P.H., Kratt, C., Dering, G., Edwards, J., Mayhew, B., McLachlan, H., 2011, Assessment of Favorable Structural Settings of Geothermal Systems in the Great Basin, Western, USA, *GRC Transactions*, Vol. 35.

Gardner, J. V., Mayer, L. A., and Hughs Clarke, J. E., 2000, Morphology and processes in Lake Tahoe (California-Nevada): Bulletin of the Geological Society of America, v. 112, no. 5, p. 736-746.

Hammond, W. C., G. Blewitt, and Kreemer, C., 2011, Block modeling of crustal deformation of the northern Walker Lane and Basin and Range from GPS velocities: J. Geophys. Res., 116, B04402, doi:10.1029/2010JB007817, p. 1-28.

Howle, J.F., 2000, The Meeks Bay right lateral moraines and implications to late Pleistocene glaciations, Lake Tahoe elevations, neotectonics, and fault geometry, (abs.), Abstr. Programs-Geol. Soc. Am. 33, A67.

Howle, J. F., G. W. Bawden, R. A. Schweickert, R. C. Finkel, L. E. Hunter, R. S. Rose and B. von Twistern, 2012, Airborne LiDAR analysis and geochronology of faulted glacial moraines in the Tahoe Sierra frontal fault zone reveal substantial seismic hazards in the Lake Tahoe region, California-Nevada, USA, Bull. Geol. Soc. Am., doi. 10.1130/830598.1

Hunter, L. E., J. F. Howle, R. S. Rose, and G. W. Bawden, 2011, LiDAR-assisted identification of an active fault near Truckee, California, Bull. Seis. Soc. Am., 101, pp. 1162-1181.

Hyne, N. J., Chelminski, P., Court, J. E., Gorsline, D. S., and Goldman, C. R., 1972, Quaternary History of Lake Tahoe, California-Nevada: Geological Society of America Bulletin, v. 83, no. 5, p. 1435-1448.

Kent, G. M., Babcock, J. M., Driscoll, N. W., Harding, A. J., Dingler, J. A., Seitz, G. G., Gardner, J.V., Mayer, L. A., Goldman, C. R., Heyvaert, A. C., Richards, R. C., Karlin, R., Morgan, C.W., Gayes, P.T., and Owen, L.A., 2005, 60 k.y. record of extension across the western boundary of the Basin and Range province: Estimate of slip rates from offset shoreline terraces and a catastrophic slide beneath Lake Tahoe: Geology, v. 33, no. 5, p. 365-368.

Lindgren, W., 1911, The Tertiary gravels of the Sierra Nevada of California: *U.S. Geol. Survey Prof. Paper 73,* p. 9-81.

Maloney, J.M., Noble, P.J., Driscoll, N.W., Kent G.M., Smith, S.B., Schmauder, G.C., Babcock, J.M., Baskin, R.L., Karlin, R., Kell, A.M., Seitz, G.G., Kleppe, J.A., 2013, Paleoseismic history of the Fallen Leaf Segment of the West Tahoe-Dollar Point fault reconstructed from slide deposits in the Lake Tahoe Basin, California-Nevada, Geosphere, v. 9, no. 4, p. 1065-1090. doi: 10.1130/GES00877.1.

Saucedo, G. J., Little, J. D., Watkins, S. E., Davis, J. R., Mascorro, M. T., Walker, V. D., and Ford, E. W., 2005, Geologic map of the Lake Tahoe Basin, California and Nevada: California Geological Survey, Regional Geologic Map No. 4, scale 1:100,000.

Schweickert, R. A., Lahren, M. M., Smith, K., and Karlin, R., 1999, Preliminary fault map of the Lake Tahoe basin, California and Nevada: Seismological Research Letters, v. 70, p. 306-312.

Schweickert, R. A., Lahren, M. M., Smith, K. D., Howle, J. F., and Ichinose, G. A., 2004, Transtensional deformation in the Lake Tahoe region, California and Nevada, USA: Tectonophysics, v. 392, no. 1-4, p. 303-323.

Smith, S. B., Karlin, R. E., Kent, G., Seitz, G., and Driscoll, N. W., 2013, Holocene Submarine Paleoseismology of Lake Tahoe: Geological Society of America Bulletin, v. 125, no. 1-2.

Tahoe Regional Planning Agency (TRPA), 2010, Lake Tahoe Basin LiDAR: http://dx.doi.org/10.5069/G9PN93H2 (October 2011).

Unruh, J., Humphrey, J., and Barron, A., 2003, Transtensional model for the Sierra Nevada frontal fault system, eastern California: Geology, v. 31, no. 4, p. 327-330.

Watershed Sciences, 2010, LiDAR Remote Sensing, Lake Tahoe Watershed, prepared for the Tahoe Regional Planning Agency, January 31, 2011.

Wesnousky, S. G., Bormann, J. M., Kreemer, C., Hammond, W. C., and J. N. Brune (2012), Neotectonics, Geodesy, Seismic Hazard in the northern Walker Lane of Western North America: Thirty kilometers of crustal shear and no strike-slip? Earth and Planetary Science Letters, 329-330, 133-140